JOURNAL OF MATERIALS SCIENCE 27 (1992) 4625–4632

Ammonia plasma treatment of ultra-high strength polyethylene fibres for improved adhesion to epoxy resin

Z.-F. LI, A. N. NETRAVALI*, W. SACHSE‡
*Department of Materials Science and Engineering, *Fiber Science Program, and ‡Department of Theoretical and Applied Mechanics, Cornell University, Ithaca, NY 14853, USA*

A study of the effect of plasma treatments on the mechanical properties and adhesion of ultra-high strength polyethylene fibres to epoxy resin is reported. Fibres were treated with ammonia plasma under various time and power conditions. The fibre/matrix interfacial shear strength was measured using load and fibre pull-out data obtained in a single-fibre pull-out test. The debonding was optically as well as acoustically monitored. Optical birefringence patterns were visible at the fibre debond region. Acoustic emission signals generated from debonding and stick–slip processes were also detected. A more than four-fold increase in the interfacial shear strength was achieved by plasma treating the fibres at the discharging condition of 30 W and 0.5 torr for 1 min. The birefringence patterns showed, qualitatively, that the shear in the matrix around the fibres increased for treated fibres and extended further into the matrix material. Surface topography of the pulled out fibres showed that the failure mode was unchanged by the treatment.

1. Introduction

For the past three decades, most advanced polymer composites have been fabricated with reinforcing fibres such as carbon, glass, and aramid. Recently, however, ultra-high strength polyethylene (UHSPE) fibres have been introduced, which possess higher specific strength, fracture toughness and chemical resistance than carbon, glass, or Kevlar^{R} fibres. For these reasons, they are being considered as replacements for a number of reinforcing fibres for composites [1, 2]. However, their low melting point, high creep, and most importantly, their poor adhesion to many matrix materials may limit their application. The creep properties of these fibres can be improved by cross-linking the polymer molecules through radiation exposure [3] or by further increasing their molecular weight or by using copolymers [4]. Such modifications usually also result in a very slight increase in the melting temperature of the fibres. In order to enhance the adhesion of UHSPE fibres to various matrix materials, modification of the fibre surface has been considered by a number of investigators [5–10].

UHSPE fibres are chemically inert and for this reason, few chemical modifications have been attempted. Such efforts have met with mixed success. Two approaches that have been explored are the chemical oxidation of the fibre by chromic acid [5] and the sulphonation of the fibre with sulphonic acid [6]. Unfortunately, such chemical treatments invariably result in a serious degradation of fibre strength [5, 6]. Plasma surface treatments for chemically inert materials have also been investigated with some success [7–11]. In a plasma process, gas molecules are dissociated into an equal number of ions and electrons, free radicals and some neutral species under a strong electromagnetic field [12]. The resulting species are highly energetic and can readily react with the substrate, modifying its surface. They can also react among themselves to create new chemical species. In addition, ultraviolet radiation is also present in the plasma [12]. Nguyen and co-workers have reported the plasma treatment of UHSPE fibres with a number of unspecified gases [7, 8]. Their results showed a two- to four-fold increase in the interlaminar shear strength and flexural strength for UHSPE fibre/epoxy composites with no significant decrease in the fibre strength.

In order to graft amine groups on to the surface of UHSPE fibres so that they can react with epoxies to form chemical bonds at the interface between fibres and epoxy resins, Holmes and Schwartz [9] treated the UHSPE fabrics using an ammonia plasma. They found that fabrics treated by ammonia plasma became completely epoxy wettable. They also found that the interfacial adhesion strength, as determined by a T-peel test, increased by 40% when the fabrics were exposed to the plasma for 5 min at a plasma power input of 50 W. Recently, Li and Netravali [10, 11] deposited UHSPE fibres with allylamine plasma-formed polymers. Their results showed that the plasma treatments improved the interfacial bond strength between the UHSPE fibres and the epoxy matrix by a factor of three or more without significantly affecting the fibre's modulus or strength [11].

0022–2461

The presence of primary amine groups after such treatments was confirmed by dye ion exchange tests [9] and by infrared spectroscopy and electron spectroscopy for chemical analysis (ESCA) measurements [10]. Ammonia plasma treatments have also been carried out on Kevlar^{R} fibres by Allred *et al.* [13]. They found a similar improvement in the adhesion of these fibres to the epoxy resins.

In this paper, we present an experimental investigation of the effects of ammonia plasma treatment on the interfacial bond strength of UHSPE fibres embedded in a DGEBA-based epoxy resin. The single-fibre pull-out technique was used to determine the interfacial bond strength. Polarized light microscopy and acoustic emission (AE) methods were used to detect and evaluate the fibre debonding and pull-out mechanisms.

2. Experimental procedure

2.1. Specimens

Ultra-high strength polyethylene fibres (Allied Signal, Spectra^{R}-900), DGEBA-type, epoxy resin, DER 331, and tetraethylene pentamine (TEPA) curing agent, DEH 26 (Dow Chemical), were used according to their manufacturer's instructions.

The silicone rubber mould used to cast the UHSPE/epoxy pull-out specimens is shown in Fig. 1a. To prepare a specimen, a fibre was mounted in the central grove of the mould and then the epoxy–hardener mixture was poured around it and cured in an oven at 100 °C for 4 h. After hardening, the protruding portion of the fibre at the lower end was sheared off using a razor blade. The diameters of individual fibres were determined using the vibroscope method according to ASTM standard, D1577-79. In these determinations, the fibre cross-section was assumed to be circular and a fibre density of 0.97 g cm^{-3} was used.

Single-fibre pull-out specimens, which permitted the observation of birefringence patterns at their fibre/matrix interface, were made in a silicone mould shown in Fig. 1b. To obtain a variation of adhesion strengths, the fibres were embedded with different embedment lengths into the epoxy resins. The test specimens were carefully polished using metallographic techniques to obtain two flat sides on each specimen. Great care was taken during polishing to avoid disturbing the free portion of the fibre. Polishing was necessary in order to be able to observe the debonding process under an optical microscope.

Anhydrous ammonia gas plasma treatments were carried out in a plasma discharge system (LFE Corporation, Model 504). This system is an inductively coupled system, operating at 13.56 MHz and consisting of four tube-type quartz vacuum reaction chambers, each approximately 130 mm diameter and 180 mm long. Prior to introducing the ammonia gas into the reaction chambers, the system was evacuated to 60 mtorr (1 torr = 133.322×10^{-2} Pa). Ammonia gas was then introduced into the chambers until the required vacuum was reached. This was maintained during the plasma discharge process by adjusting the flow rate.

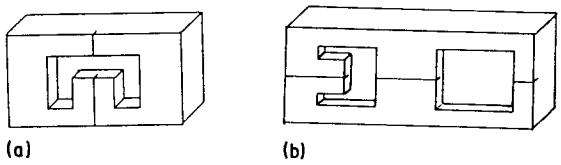

Figure 1 (a) Silicone rubber mould for moulding the pull-out specimens. (b) Silicone rubber mould and specimen for observation of pull-out process using optical microscopy.

2.2. Single-fibre tensile tests

The strength of the fibres was determined using a mechanical tensile testing machine (Instron Model 1122) operating at a crosshead speed of 5 mm min^{-1}. To prevent slippage of the fibre in the clamps, the ends of the fibre were wound on to small capstan clamps [14]. The nominal gauge length between the two clamps was 50 mm. For each experimental condition, 25 fibres were tested. The measured failure stresses were fit to a two-parameter Weibull distribution whose shape and scale parameters were obtained using a maximum likelihood estimation technique [15].

2.3. Single-fibre pull-out test

The apparatus used to perform the single-fibre pull-out test is shown schematically in Fig. 2. The pull-out tests were carried out at a crosshead speed of 1 mm min^{-1}. Ten single-fibre pull-out tests were conducted for each experimental condition. The average interfacial shear strength (IFSS) was evaluated according to the following equation:

$$\text{IFSS} = \frac{\sigma_p r}{2l} \quad (1)$$

where σ_p is the peak stress of pull-out, r is the radius of the fibre, and l is the embedded length of the fibre.

A number of single-fibre pull-out specimens were also immersed in hot water at 70 °C for 5 h and then placed in cold tap water for 15 min. After taking the specimens out of water and wiping away the excess

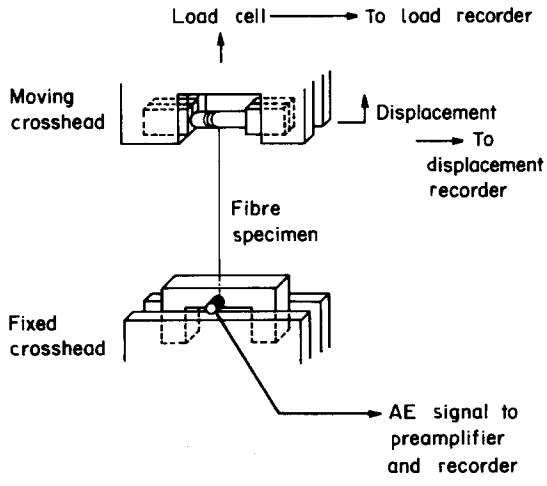

Figure 2 Schematic drawing of the single-fibre pull-out test.

water with a soft tissue, the single-fibre pull-out tests were conducted.

To test a specimen, it was mounted into a straining frame and the load applied via the testing machine. The pull-out process was monitored with an optical microscope, equipped with a cross-polarizer. Acoustic signals (AE) emitted during the loading and detected with a miniature piezoelectric sensor of aperture 1.3 mm attached to the side of the specimen were also recorded during the pull-out process. The sensor output was amplified from 40 dB to 100 dB using one or more low-noise, broadband pre-amplifiers. The signals were input to a waveform recorder which, in turn, was connected to a signal acquisition and processing system.

3. Results and discussion

3.1. Fibre characterization

The fracture strength, the fracture strain and modulus data determined for single fibres subjected to different plasma treatments are presented in Table I. It is seen that for a plasma generated at a constant power input of 30 W, the fibre strength increases for treatment times up to 30 s, but decreases slightly for longer times. However, after 25 min treatment, the strength does not decrease significantly. For a fixed treatment time of 5 min, the fibre strength increases with low power levels such as 20 W, and it decreases with higher input powers. Strength loss becomes significant above 65 W. It has been argued that electron and gamma radiation cause both cross-linking and chain scissions in disordered regions while causing only chain scissions and structural degradation in the crystalline region of the fibre [3]. It is recognized that microstructural changes resulting from the plasma treatment occur only in the outer few molecular layers of a specimen [16].

As discussed earlier, a plasma contains electron and ultraviolet radiation [12]. Previous work has shown that the electron density increases with power input [12]. At lower power inputs and short treatment times, the radiation effect on the strength degradation in the crystalline region is less significant than the effect of cross-linking at the amorphous region, which leads to an increase in overall fibre strength and a significant increase in modulus. According to the structural model proposed by Grubb [17] for high-modulus polyethylene fibres, the modulus of fibre can be expressed by

$$E = b\left(\frac{1-f}{E_c} + \frac{f}{E_e}\right)^{-1} + (1-b) \times \left[\frac{x-(1-f)b}{(1-b)E_c} + \frac{1-x-fb}{(1-b)E_a}\right] \quad (2)$$

where E_c, E_a, and E_e are, respectively, the moduli of the crystalline region, the amorphous region and the entanglement region, x is the crystallinity fraction, b is the structural model factor, and fb is the volume fraction of entanglement region. For shorter times and lower power inputs, both E_a and E_e increase, while E_c is not significantly affected, which, according to Equation 2 leads to a significant increase in the fibre modulus. For treatment times exceeding 30 s and power inputs higher than 65 W, the fracture strains increase, while the fracture strengths and moduli decrease, suggesting chain scissions occurring in the crystalline regions which lower the E_c values.

The fibre surface topography was examined using a scanning electron microscope (SEM). Fig. 3a and b show scanning electron micrographs of a control fibre and a treated fibre, respectively. It appears that the ammonia plasma treatments used in this study, i.e. 100 W for 5 min and 30 W for 25 min, result in no apparent etching of the surface of the fibres. Holmes and Schwartz, who used an ammonia plasma to treat UHSPE fabrics, reported similar observations on their fibres [9]. These observations are in contrast with the cellular texture observed by Ladizesky and Ward who used an oxygen plasma treatment on their fibres [5]. This treatment resulted in a severe etching of the fibres.

TABLE I Effect of ammonia plasma treatments on fibre mechanical properties

Plasma treatment conditions			Fibre properties				
Power (W)	Pressure (torr)	Time (min)	Strength			Strain (%)	Initial modulus (GPa)
			Mean (MPa)	Scale parameter (MPa)	Shape parameter		
Control			3530	3635	16.7	5.32	66.6
30	0.5	1/6	3673	3818	13.2	4.93	75.9
30	0.5	1/2	3737	3904	11.4	4.54	100.9
30	0.5	1	3318	3456	11.7	4.82	70.2
30	0.5	5	3447	3548	17.0	5.20	66.9
30	0.5	10	3564	3743	9.4	5.03	71.6
30	0.5	25	3390	3595	7.0	5.12	66.7
20	0.5	5	3725	3833	18.6	4.60	99.6
30	0.5	5	3447	3548	17.0	5.20	66.9
65	0.5	5	3322	3466	11.6	4.80	69.6
100	0.5	5	3191	3337	10.2	4.96	65.0

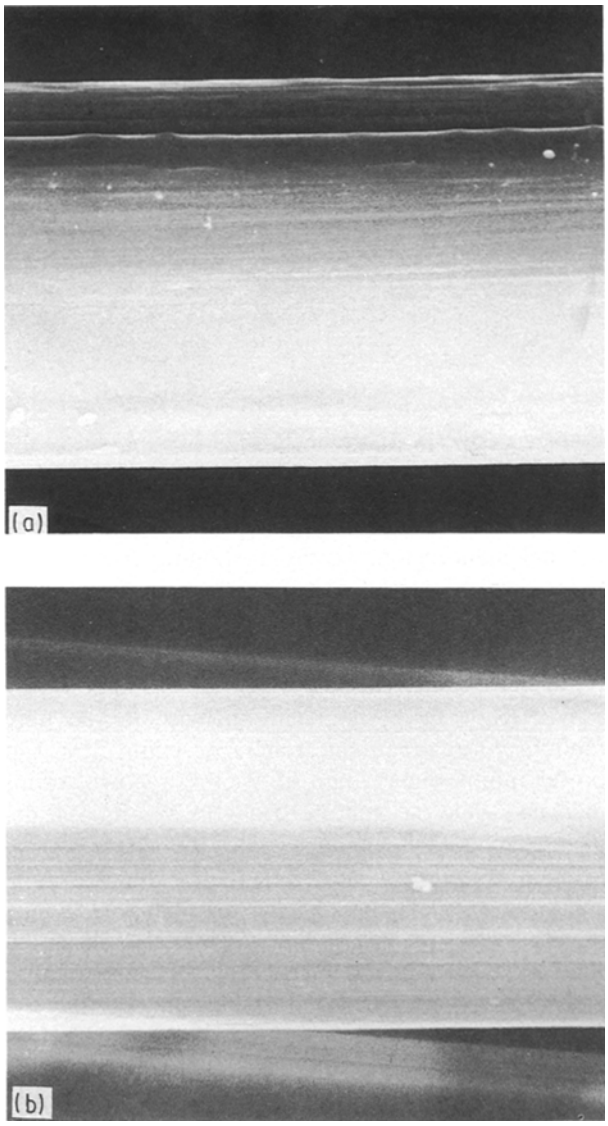

Figure 3 Scanning electron micrograph of the fibre surface. (a) Control specimen, (b) plasma-treated specimen.

3.2. Interfacial debonding and fibre pull-out

Fig. 4a–d show typical plots of stress versus displacement data obtained in single-fibre pull-out tests. Two or more stress peaks appear in every data set. Further, from optical microscopy observations it appeared that the pull-out proceeded in two phases: (1) interfacial debonding, and (2) fibre pull-out. As the fibre is loaded, shear stresses along the fibre/matrix interface increase [18, 19]. The maximum shear stress occurs at the point at which the fibre enters the epoxy matrix [20]. When the maximum shear stress reaches a critical value, debonding at the interface initiates. In practice, it is difficult to identify from the load versus displacement data the precise point at which the debonding initiates. It is therefore difficult to determine precisely the shear stress value at which debonding initiates. With further loading, the pull-out stress in the fibre continues to increase and the debonding propagates slowly along the embedded length of the fibre. In the optical photomicrograph shown in Fig. 5 the portions of the fibre bonded and debonded from the epoxy matrix can be identified. In this example, the light region surrounding the fibre on the right side corresponds to the debonded portion of the fibre, whereas the other side which is not debonded, appears as a dark region, in which it is difficult to distinguish the fibre from the matrix material. With increasing pull-out stress, the lighter area, corresponding to the debonded region, expands towards the left as the interface crack propagates. At the first peak in the load–displacement curve, the debonding of the fibre from the matrix is complete and subsequent fibre pull-out proceeds in a stick–slip mode. Each time the fibre slips, the load exhibits a sudden drop. This process has been extensively described and analysed by Chua and Piggott [18, 19]. Four distinct modes of fibre pull-out were observed with our specimens. These are illustrated in Fig. 4a–d. After the first significant drop in load, corresponding to the first peak, the load supported by the fibre increases again until it reaches the maximum static friction force. Thereafter, the fibre may be pulled out slowly and continuously as Fig. 4a illustrates, or with large or small steps of stick–slip, as the maximum friction force at the interface is exceeded. For fibres with good adhesion (Fig. 4b–d), the fibre is not pulled out continuously. Instead, the pull-out proceeds in stick–slip steps which appear as distinct load drops as shown in Fig. 4b. In some cases, the fibres are pulled out continuously after only a few stick–slip steps as shown in Fig. 4d. The number of each type of pull-out modes for all different treatments are presented in Table II. The data show that the number of stick–slip steps increases with a corresponding increase in the fibre/matrix interfacial shear strength.

3.3. Effect of plasma treatment on interfacial shear strength

The average interfacial shear strength and maximum friction force measured for each pull-out specimen are also tabulated in Table II. The average interfacial shear strengths were calculated using Equation 1 and the load value of the first peak in each test. The maximum load attained after the first peak in the load versus displacement data was taken as the maximum frictional force. It is evident from the data in Table II that significant increases in both the IFSS and the frictional force for all plasma treatments with duration greater than 10 s. Fig. 6 shows the effect of treatment time on the IFSS at a constant power level of 30 W. It is seen that the interfacial shear strength increases with treatment time but it quickly reaches a maximum value at 1 min exposure. With further increase in treatment time, the IFSS decreases. This is probably a consequence of the number of primary amine radicals which are converted to secondary and tertiary amines and other radicals [10]. It is known that the tertiary amines cannot cross-link with epoxies as the primary amines do, although they do increase the surface polarity and surface wetting [21]. It is seen that the maximum IFSS of 2.37 MPa obtained under the condition of 30 W, 0.5 torr and 1 min plasma treatment is more than four times higher than that obtained for the untreated specimens. Fig. 7 shows the effect of power input on the IFSS. With an increase in power input at

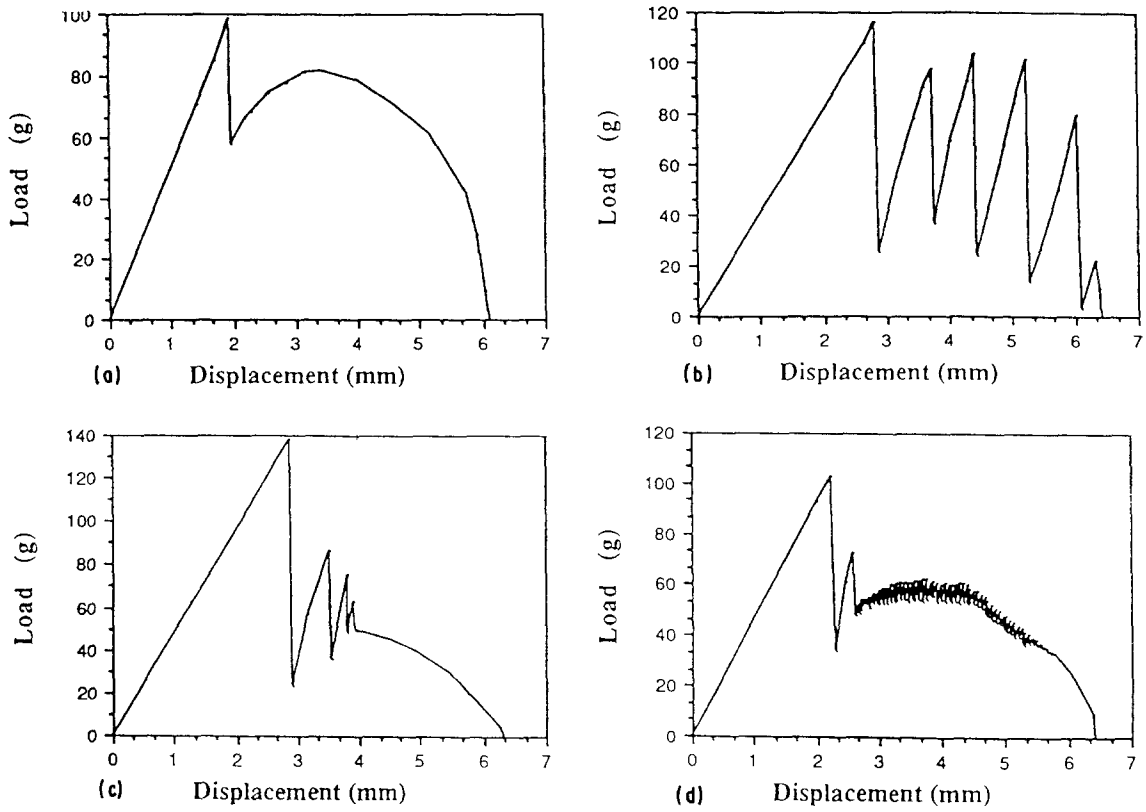

Figure 4 Different patterns of stress–displacement plots for single-fibre pull-out tests.

TABLE II Results of single-fibre pull-out tests

Plasma treatment			Interface binding properties						
Power (W)	Pressure (torr)	Time (min)	IFSS (MPa)	(CV) (%)	Max. friction (g-force)	Pull-out mode[a]			
						A	B	C	D
Control			0.56	(13.4)	39.6	10	0	0	0
30	0.5	1/6	0.77	(16.4)	43.6	10	0	0	0
30	0.5	1/2	2.16	(22.9)	110.2	1	5	2	2
30	0.5	1	2.37	(28.4)	120.6	0	10	0	0
30	0.5	5	2.09	(32.7)	89.4	0	6	4	0
30	0.5	10	1.89	(20.7)	93.9	5	5	0	0
30	0.5	25	1.64	(18.7)	89.2	5	0	3	2
20	0.5	5	1.97	(18.8)	90.0	7	3	0	0
30	0.5	5	2.09	(32.7)	89.4	0	6	4	0
65	0.5	5	1.99	(10.9)	103.6	3	3	3	1
100	0.5	5	1.48	(30.6)	71.8	2	1	5	2

[a] ABCD refer to the modes shown in Fig. 4a–d, respectively.

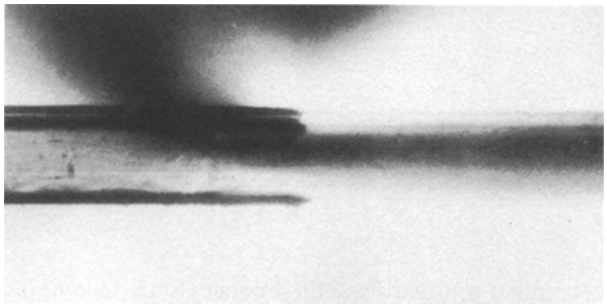

Figure 5 Optical photo-micrograph showing the propagation of debonding along the interface for a plasma-treated fibre. The dark line indicates the debonded part of the fibre.

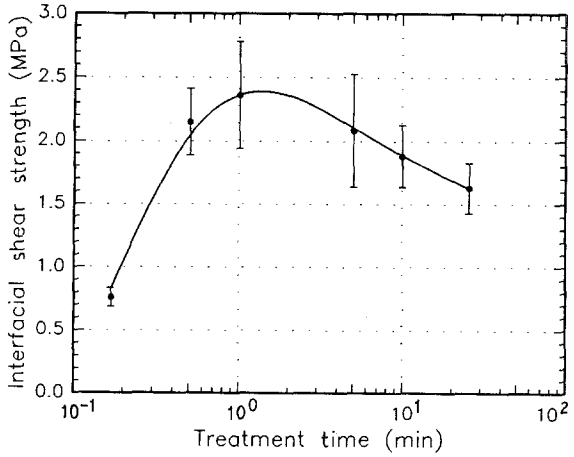

Figure 6 Effect of ammonia plasma treatment time on the interfacial shear strength. Constant plasma power, 30 W; chamber pressure, 0.5 torr.

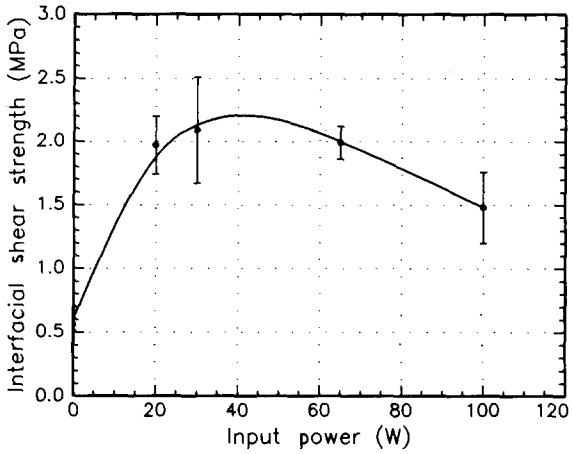

Figure 7 Effect of ammonia plasma input power on the interfacial shear strength. Treatment time, 5 min; chamber pressure, 0.5 torr.

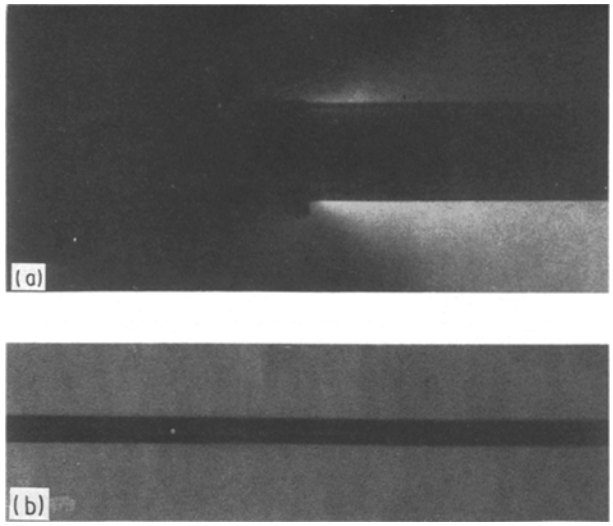

Figure 8 Polarized light photo-micrograph showing the interfacial shear stress along the bonded fibre near the debonded region. (a) Plasma-treated fibre, (b) control fibre.

the same pressure (0.5 torr), the IFSS values increase and reach a maximum at a power level of 30 W. Further increases in the power input result in a decrease of the IFSS values. A possible explanation of this observation is that at higher power levels, more energy is available to break the ammonia molecules into ions or smaller free radicals which make it difficult to obtain higher primary amine group concentrations. Consequently, the IFSS values decrease from their peak values, though they remain higher than the values measured for specimens containing untreated fibres.

The improvement in interfacial shear strength can be visualized in the shear stress-induced, photoelastic birefringence patterns in the matrix material surrounding a fibre. A shear stress in the matrix material results in an alignment of the epoxy molecular chains in the direction of stress, creating a birefringence pattern. When this is viewed under cross-polarizers, a pattern, like that shown in Fig. 8a can be seen. For untreated fibres, the IFSS is too small to create any appreciable shear stress around the fibre which would result in an alignment of the molecular chains. In such a case, no photoelastic fringes can be seen as illustrated by Fig. 8b. Fig. 9a and b are scanning electron micrographs of the embedded portions of the control and plasma-treated fibres which have been pulled-out of the epoxy resin. The fibre surfaces appear to be clean for both treated and untreated fibres, indicating that the debonding occurred solely at the interface.

For the single-fibre pull-out specimen immersed in hot water of 70 °C for 5 h, the interfacial shear strength of untreated specimens was reduced by 66%. In contrast, for specimens containing plasma-treated fibres, the IFSS dropped by only 7%. These preliminary results suggest that a well-bonded interface is better able to resist diffused water.

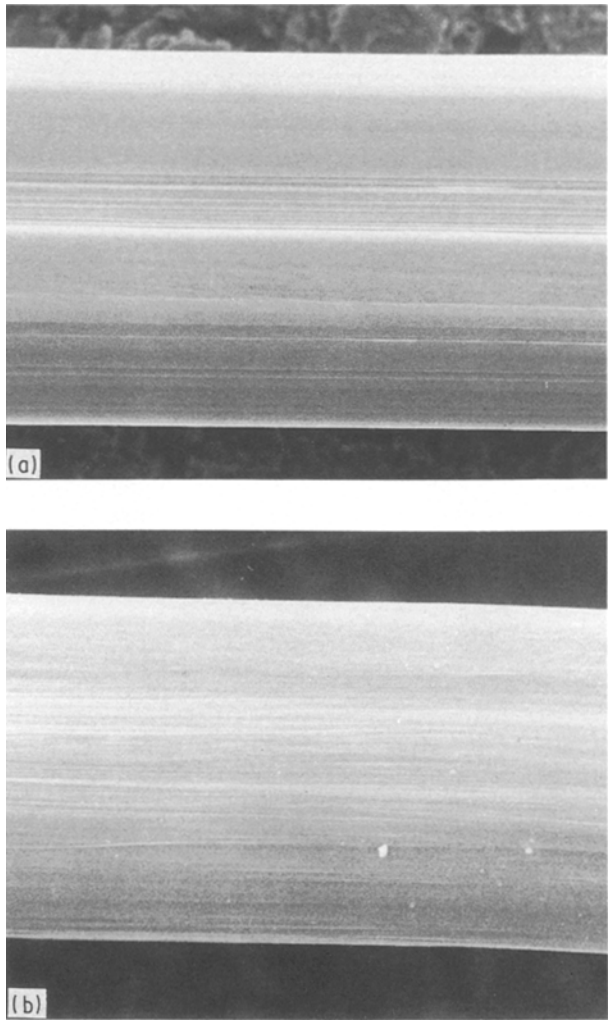

Figure 9 Scanning electron micrograph of the fibre surface pulled from epoxy resin. (a) Control fibre, (b) plasma-treated fibre.

3.4. Acoustic emission from single-fibre pull-out

The load versus displacement records of Fig. 4 show that there appear one or more peaks in the load during the pull-out process. These correspond to fibre debonding and subsequent slippage. Such instantaneous releases of stress and energy can be a source of acoustic signals which when propagated from the source location to the surface of the specimen, can be

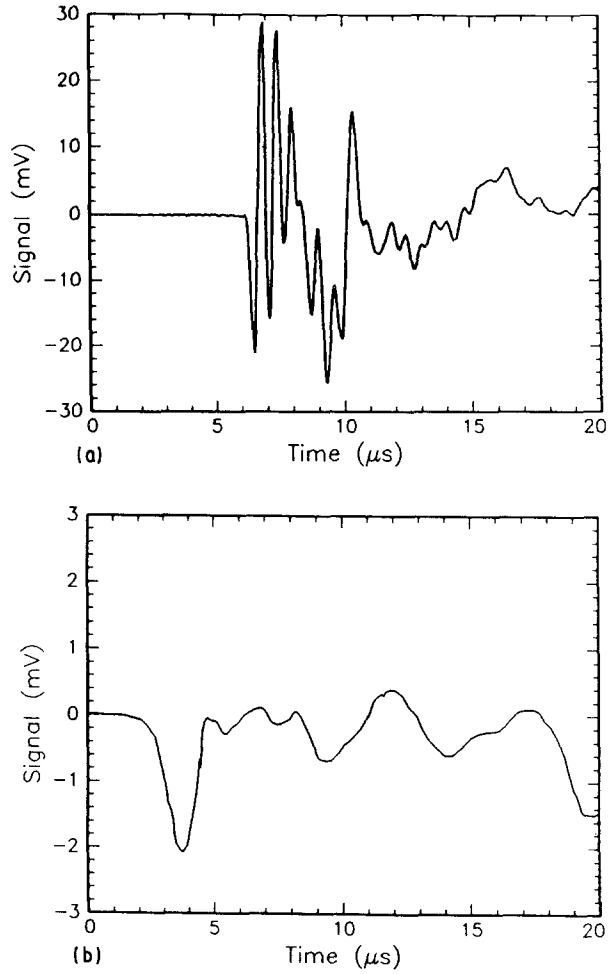

Figure 10 AE signals from single-fibre pull-out for a plasma-treated fibre. (a) First fibre pull-out signal, (b) fibre sliding signal.

detected as AE signals. It was difficult to detect AE signals from specimens fabricated with an untreated fibre. This indicates that the energy released during the debonding of such fibres from the matrix was so small that the signals at the ultrasonic sensor were less than the system's signal detection threshold, which was estimated to be about 2 μV. For treated fibres, several signals could be detected. These are shown in Fig. 10a and b. It was observed that the first detected AE signal always corresponded to the first stress drop corresponding to a complete fibre/matrix debonding and this signal was the highest amplitude AE signal observed during the test. Subsequent signals, corresponding to the fibre pull-out, were far lower in amplitude and highly variable. Additional experiments, possibly with a more advantageous testing geometry and an array of sensors will be required if the connection between fibre/matrix failure and emitted acoustic signals is to be unambiguously determined.

4. Conclusion

Experiments investigating the effect of ammonia plasma treatment on UHSPE fibres and their interfacial strength under different experimental conditions have been described. The ammonia plasma treatment was found to increase the interfacial shear strength of UHSPE fibres in an epoxy matrix. At a medium power level of 30 W and extended periods of treatment time, the strength and fracture strain of the fibres appear to be unaffected. However, at power levels above 65 W, the fibre strength decreases significantly.

The IFSS of UHSPE fibres embedded in an epoxy matrix increased for all experimental conditions. At a plasma input power level of 30 W, the IFSS increased with treatment time. It reached a maximum of 2.37 MPa for a 1 min treatment. This corresponds to a four-fold increase over the untreated fibres. With further increase in treatment time, up to 25 min, the IFSS decreased steadily. For a fixed treatment time of 5 min, the IFSS reached a maximum at 30 W power and fell with further increase in power level. From photoelastic birefringence patterns it appears that an increase in the IFSS is accompanied by shear stresses surrounding a loaded fibre extending further into the matrix. The topography of failed fibre surfaces showed no appreciable change after the treatment.

Once the interface failed, the fibre pull-out proceeds in a stick–slip mode. Four different types of load–elongation curves were observed. In the case of fibres with lower IFSS, the stick–slip steps were small or essentially non-existent. For fibres with higher IFSS, large steps were seen. Acoustic emission signals of varying amplitudes were detected during the pull-out process.

Acknowledgements

The authors thank Professor D. T. Grubb for his encouragement of this project and the support of ZFL to complete the data analysis and the writing of this paper. This project was supported by the Materials Science Center at Cornell University which is funded by the National Science Foundation. One of the authors (W. S.) was supported, in part, by the Office of Naval Research (Solid Mechanics Program) under Grant N00014-90-J-1273.

References

1. H. W. CHANG, L. C. LIN and J. F. LINDSEY, in "31st International SAMPE Symposium", Vol. 31, Los Angeles, CA, edited by J. Bauer and R. Dunaetz (SAMPE, Covina, CA, 1986) p. 859.
2. R. S. ZIMMERMAN and D. F. ADAMS, in "32nd International SAMPE Symposium", Vol. 32, San Diego, CA, edited by R. Carson, M. Burg, K. J. Kjoller and F. J. Riel (SAMPE, Covina, CA, 1987) p. 1461.
3. D. W. WOODS, W. K. BUSFIELD and I. M. WARD, *Plastics Rubber Process. Applic.* **9** (1988) 155.
4. I. M. WARD, *Brit. Polym. J.* **18** (1986) 216.
5. N. H. LADIZESKY and I. M. WARD, *J. Mater. Sci.* **18** (1983) 533.
6. A. R. POSTEMA and A. J. PENNINGS, in "High Modulus Polymers – Approaches to Design and Development", edited by A. E. Zachariades and R. S. Porter (Marcel Dekker, New York, 1988) p. 431.
7. N. X. NGUYEN, G. RIAHI, G. WOOD and A. POURSARTIP, in "33rd International SAMPE Symposium", Vol. 33, Anaheim, CA, edited by G. Carillo, E. D. Newell, W. D. Brown and P. Phelan (SAMPE, Covina, CA, 1988) p. 1721.
8. S. L. KAPLAN, P. W. ROSE, N. X. NGUYEN and H. W. CHANG, *ibid.* (1988) p. 1721.
9. S. HOLMES and P. SCHWARTZ, *Compos. Sci. Technol.* **38** (1990) 1.

10. Z.-F. LI and A. N. NETRAVALI, *J. Appl. Polym. Sci.* **44** (1992) 319.
11. *Idem, ibid.* **44** (1992) 333.
12. H. YASUDA, "Plasma Polymerization" (Academic Press, New York, 1985).
13. P. Z. ALLRED, E. W. MERRILL and D. K. ROYLANCE, in "Molecular Characterization of Composite Interface", edited by H. Ishida and G. Kumar (Plenum Press, New York, 1985).
14. P. SCHWARTZ, A. NETRAVALI and S. SEMBACH, *Textile Res. J.* **56** (1986) 502.
15. A. C. COHEN, *Technometrics* **7** (1965) 579.
16. O. S. KOLLURI, S. L. KAPLAN and P. W. ROSE, "Gas Plasma and the Treatment of Advanced Fibers", paper presented at the Society of Plastics Engineers, "Advanced Polymer Composites 1988", Technical Conference, Los Angeles, CA, November 1988 (SPE, Brookfield, CT, 1988)
17. D. T. GRUBB, *J. Polym. Sci. Polym. Phys. Ed.* **21** (1983) 165.
18. P. S. CHUA and M. R. PIGGOTT, *Compos. Sci. Technol.* **22** (1985) 33.
19. *Idem, ibid.* **22** (1985) 185
20. A. TAKAKU and R. G. C. ARRIDGE, *J. Phys. D Appl. Phys.* **6** (1973) 2038.
21. H. LEE and K. NEVILLE, "Handbook of Epoxy Resins" (McGraw-Hill, New York, 1967).

Received 13 March
and accepted 1 July 1991